Reac Kinet Mech Cat (2017) 121:109–119
DOI 10.1007/s11144-016-1134-2

Co and Ni catalysts loaded on typical well-ordered micro- and mesoporous supports for acetic acid reduction

György Onyestyák[1] · Gyula Novodárszki[1] · Ágnes Farkas Wellisch[1] · Dénes Kalló[1] · Ashim J. Thakur[2] · Dhanapati Deka[2]

Received: 22 November 2016 / Accepted: 28 December 2016 / Published online: 4 January 2017

Abstract The consecutive reduction of acetic acid was studied over two monometallic (nickel and cobalt) catalysts compared to indium doped bimetallic composites. A fixed bed flow-through reactor was applied with hydrogen stream at 21 bar at 240–380 °C. Efficient catalysts containing finely dispersed metal particles were obtained by in situ pretreatment with H_2 at 450 °C. It was shown that cobalt, opposite to nickel, can direct the consecutive catalytic reduction to ethanol formation inhibiting hydrodecarbonylation. Resulting in higher activity, the well-ordered mesoporous silica, SBA-15 seems to be more efficient support than a crystalline microporous aluminosilicate, FAU.

Keywords Acetic acid reduction · Ethanol production · Cobalt catalysts · X,FAU · SBA-15

Introduction

In some biomass degradation pathways, carboxylic acids are produced. Volatile fatty acids are considered as platform molecules of the chemical industry [1]. The alcohols obtained by the selective reduction of these acids can be used mainly as biofuel. The process of bioacid hydroconversion requires novel, more efficient catalysts. Bimetallic contacts often show enhanced activity, higher selectivity and better stability relative to the single metal forms, containing any of the component metals. These properties made bimetallic catalysts useful to convert materials of

✉ György Onyestyák
onyestyak.gyorgy@ttk.mta.hu

[1] Research Centre for Natural Sciences, Institute of Materials and Environmental Chemistry, Hungarian Academy of Sciences, Magyar Tudósok körútja 2, Budapest 1117, Hungary

[2] Biomass Conversion Laboratory, Department of Energy, Tezpur University, Tezpur, Assam 784028, India

biomass origin to fuels and chemicals [2]. From the 1960s, as a result of the extensive investigations, bimetallic catalysts became widely utilized in many catalytic applications. The effect of Sn additive, for example, on the catalytic properties of Pt/alumina has been reported in numerous studies [3], whereas the promoting effect of the indium, neighbor of tin, received much less attention [4–6].

The hydrogenolysis of C–C bonds is the dominant process of carboxylic acid hydroconversion over some monometallic catalysts, such as noble metals or nickel. Over these catalysts, hydrodecarbonylation proceeds but hardly any alcohol formed. The indium additive drastically changes the catalytic mechanism, eliminating C–C bond cleavage [7, 8] completely. In such cases, the carboxylic acid is converted in consecutive hydrogen addition/dehydration/hydrogen addition steps resulting finally in the selective formation of alcohol.

In the nickel-indium bimetallic catalysts, the Ni_2In phase was found to be present substantiating that this phase was responsible for the significant improvement of alcohol selectivity and yield relative to the corresponding properties of the monometallic forms [7, 9]. Regarding the catalytic behavior, the structure and composition of the metal particles are of decisive importance, which is affected to some extent by the structure and composition of the support. Thus, the activity of the catalyst is profoundly influenced by the support [10]. The present work shows the importance of the support properties by comparing highly ordered mesoporous silica, SBA-15, and a microporous zeolite, faujasite structures as supports of nickel, cobalt, nickel-indium and cobalt-indium hydrogenating active phases. For example, the less active copper on SBA-15 became much more active, approaching nearly the catalytic properties of the most effective Ni-forms, similarly loaded on this mesoporous material, characterized by low diffusional resistance [11]. In the present work, investigation and comparison of cobalt as the left neighbor of nickel in the periodic table is initiated.

Experimental

Materials

Supported Ni, Co and NiIn, CoNi catalyst precursors were prepared and converted to metallic catalyst by reduction with H_2 before use both in the high-temperature X-ray diffraction cell (XRD) and in the high-pressure catalytic reactor.

Silica supported Ni or Co catalyst precursors, containing 9 wt% metal, were prepared by the incipient wetness impregnation of silica support with NH_3 solution (Reanal, Hungary) of Ni or $Co(acetate)_2$ (Aldrich), dried at 120 °C and calcined at 400 °C in air stream. Amorphous silica SBA-15 was applied as a catalyst support containing hexagonally ordered, uniform, parallel mesopores of about 6 nm diameter. It was synthesized by a sol–gel method using an amphiphilic triblock copolymer Pluronic P123 as organic structure-directing agent [12]. The specific surface area (SSA) of the material, determined by the BET method, was 893 m^2/g.

Nickel or cobalt faujasite catalyst precursors were prepared from NaX (product of the late VEB CKB, Bitterfeld-Wolfen, Germany) powder by conventional

aqueous ion-exchange using nickel(II) or cobalt(II) acetate solutions. A slurry of zeolite and an aqueous Ni^{2+} or Co^{2+} acetate solution, having a liquid to solid weight ratio of 10, was stirred at room temperature. The amount of metal cation in the slurry was equivalent with the ion-exchange capacity of the zeolite. After 8 h of stirring, the solid and the solution were separated and the exchange procedure was repeated using a fresh solution. The solid was separated again, washed three times with distillated water, and finally dried at room temperature. The obtained zeolites, NiX and CoX contain $\sim$9 wt% metal.

Bimetallic catalyst precursors were prepared by adding indium(III) oxide (Aldrich) to precursors of Ni or Co catalysts in amounts to attain Me_2In stoichiometric composition of the metallic phase. The mixture was then grinded in an agate mortar.

The same designation was used for the catalyst precursor and the corresponding catalyst, containing the symbol of the metal(s) and the name of the support, such as, NiX, NiInX, Ni/SBA-15, NiIn/SBA-15, CoX, CoInX, Co/SBA-15 and CoIn/SBA-15.

Methods

The catalyst precursor was loaded into a high-pressure, fixed bed, flow-through reactor and reduced in a flow of 100 cm^3/min pure hydrogen in situ in the reactor at 450 °C and 21 bar for 1 h to obtain active supported metal catalyst. The hydrogenation of acetic acid (AA) (96%, Reanal, Hungary) was studied at 21 bar total pressure in the temperature range 220–380 °C. The reactor effluent was cooled down to room temperature, the liquid and gaseous products were separated. The liquid was analyzed using a gas chromatograph (Shimadzu 2010) equipped with a Restek Rt-U-BOND capillary column, and a flame ionization detector. The gas was analyzed on-line by a gas chromatograph (HP 5890) equipped with Carboxen 1006 PLOT capillary column and thermal conductivity cell. The product distributions are represented as stacked area graphs (unusual but more expressive plotting) where the distance between two neighboring curves represents the yield of a given product in mole percent.

XRD patterns of the catalysts were recorded at elevated temperatures in hydrogen flow using a high-temperature XRD cell in a Philips PW 1810 diffractometer. The mean crystallite size of the metal particles was calculated by the Scherrer equation. The morphological analysis of the samples was carried out with a FEI Morgagni 268D type TEM. Adsorption isotherms of nitrogen were determined at −196 °C using Quantochrome Autosorb 1C sorptometer.

The reducibility of the samples were examined by temperature-programmed H_2-reduction (H_2-TPR) using a flow-through quartz microreactor. About 30 mg catalyst was pretreated in a flow of 30 ml/min nitrogen at 450 °C for 1 h. The pre-treated sample was then cooled to room temperature in the same N_2 flow before contacted with a 30 cm^3/min flow of 9.7% hydrogen containing H_2/N_2 mixture. The reactor temperature was ramped up at a rate of 10 °C/min to 800 °C and maintained for 1 h at this temperature. The effluent gas was passed through a liquid nitrogen trap and a thermal conductivity detector (TCD). Calculation of the corresponding hydrogen

consumptions based on the peak areas was carried out by using the calibration value determined with the H_2-TPR of CuO reference material.

Results and discussion

The type I N_2 physisorption isotherm of the reduced zeolite CoX sample is shown in Fig. 1. The zeolite structure of the Ni(X) or CoX preparations is more resistant during hydrogen reduction than that of zeolites CuX, CuA and CuP [13] because of higher reduction temperature of Co and Ni cations. Thus charge compensating protons appear only to a lower extent at the routine pretreatment temperature (450 °C) and in already highly dehydrated zeolites.

The adsorption isotherms of the SBA-15 samples are also shown in Fig. 1. The isotherms of the reduced Ni- or Co-containing SBA-15 samples were found nearly identical, therefore, only the isotherm of the Co/SBA-15 sample is shown in the present work. The isotherms of SBA-15 samples are of type IV with H2 hysteresis loop. The mean diameter of the mesopore is approximately 6 nm. The conventional

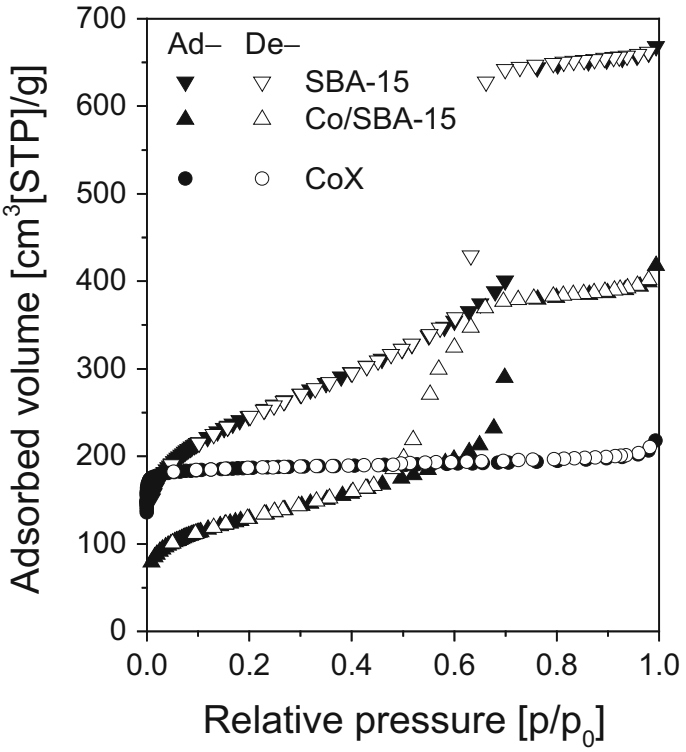

Fig. 1 Isotherms of nitrogen adsorption (*full symbols*) and desorption (*open symbols*) at −196 °C of CoX (*filled circle*, *open circle*) zeolite, SBA-15 (*filled inverted triangle*, *open inverted triangle*) and Co-loaded SBA-15 (*open triangle*, *filled triangle*) materials after treatment in H_2 flow at 21 bar and 450 °C for 1 h

incipient wetness capillary impregnation technique resulted in cobalt or nickel oxide particles in the channels. Upon H_2 reduction at temperatures above the melting point of the indium metal, mobile indium atoms are formed from the In_2O_3. These atoms can easily reach the particles of main metals formed in the channel and can generate alloys. The formation of metal particles partly blocking the parallel mesopores resulted in catalyst having smaller SSA (between 440 and 480 m^2/g) than the parent SBA-15 material. The metal particles inside the channels can be seen in the TEM images of Fig. 2 (shown only for Ni-containing samples). An investigation of the Co-samples showed that it was impossible to obtain images with acceptable quality. However, measuring almost the same isotherms, similar images can be figured. The longer particles of the intermetallic compound Ni_2In detected by XRD are also observable on the TEM image of the catalyst (see right side of Fig. 2). The metal and the alloy particles fully block short sections of the channels, being responsible for the lower SSA of the SBA-15 catalysts that of the pure support.

H_2-TPR fingerprints demonstrate that the evolution of active metallic phases (Co^0 or Ni^0) during reduction by H_2 (results shown in Fig. 3 only for Co-forms, because the H_2-TPR curves obtained on Ni-samples were hardly different) from the oxides formed upon the calcination of the acetate-impregnated SBA-15 material is already highly progressed at 450 °C (routine pretreatment temperature before the reaction). On the contrary, cations of cobalt or nickel as charge compensating species are localized on sites determined by the zeolite structure and are situated in a strong electrostatic field. However, this technique can gives only qualitative information about reducibility of different agents.

The HT-XRD technique is really proven powerful parallel to dynamic methods as H_2-TPR (see the HT-XRD patterns in Fig. 4). The NiO formed during calcination of impregnated Ni-acetate can be fully reduced to nickel leaving enough time for reduction at selected temperatures keeping constant for 30 min below 450 °C (the routine pretreatment temperature prior to catalytic investigations) (see in curves a and c in Fig. 4A). Half an hour was found to be sufficient for the total reduction of the investigated samples on a high enough temperature. For cobalt, the situation is similar (see Fig. 4a). The average size of Ni^0 particles in the Ni/SBA-15 catalyst, estimated by the Scherrer equation was 21 nm. This infers that short metal

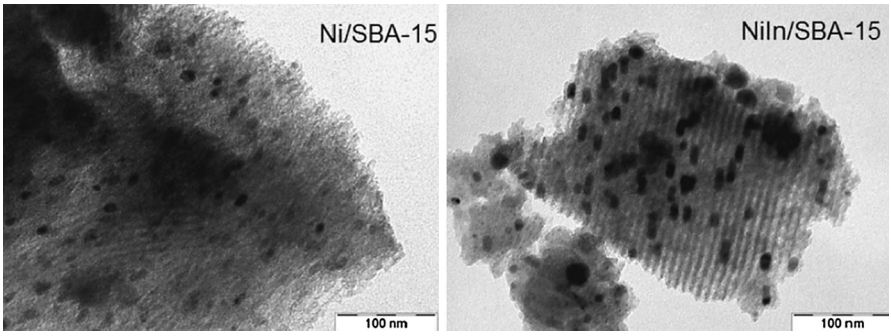

Fig. 2 TEM images of the SBA-15 supported mono- and bi-metallic nickel catalysts after treatment in H_2 flow for 30 min at 450 °C

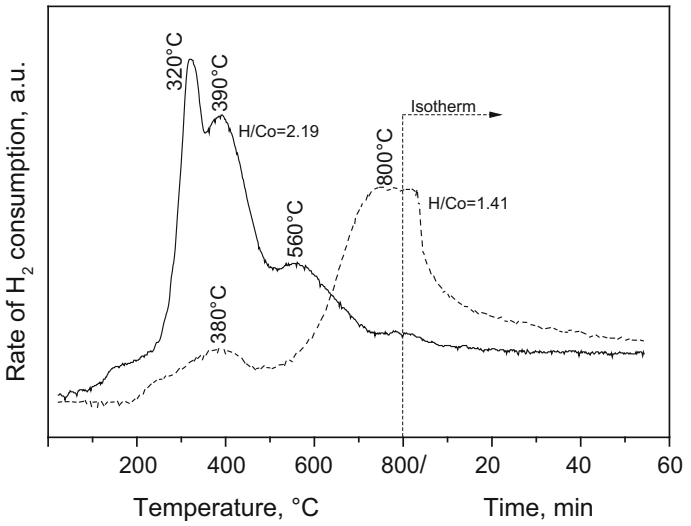

Fig. 3 H_2-TPR of Co-cations supported on X-faujasite (*dashed line*) and SBA-15 silica (*solid line*)

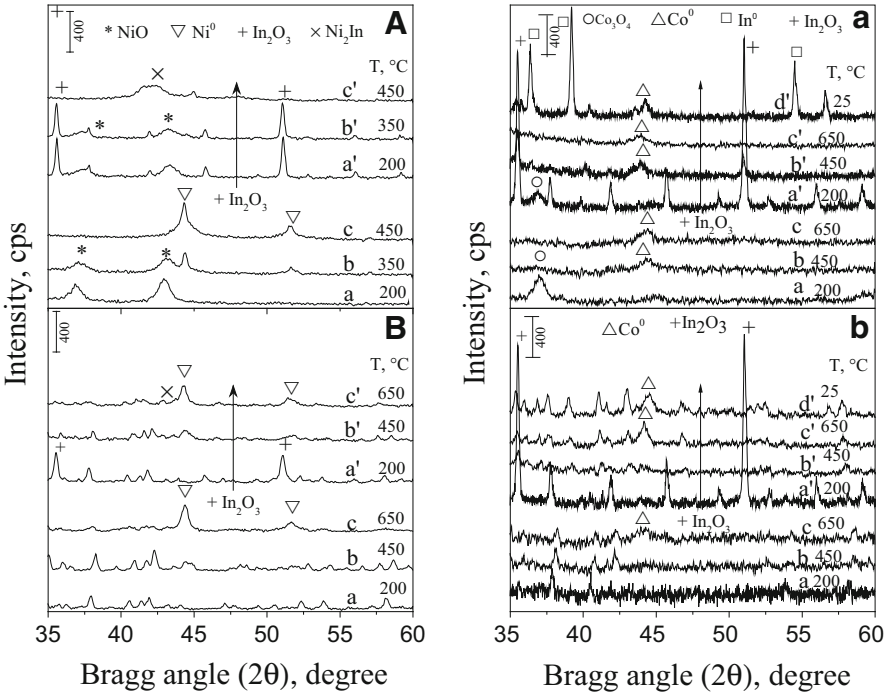

Fig. 4 HT-XRD patterns of SBA-15 (**A**, **a**) and zeolite X (**B**, **b**) supported Ni (**A**, **B**) and Co (**a**, **b**) catalysts recorded in H_2 flow. Indium doping was carried out with admission of 10 wt% In_2O_3 (40 wt% with Co/SBA-15/a/). The materials were kept at the indicated temperature for 30 min before recording a diffractogram

nanowires could have been formed instead of spheres because of the spatial constraints posed by the channels of 6 nm diameter (see Fig. 2). Cobalt particles were found to be much smaller (11 nm). The larger active metal surface is advantageous resulting in higher activity, so lower reaction temperature is needed when the selectivity may be better.

In the presence of In_2O_3, one of the Ni-In intermetallic compounds (Ni_2In) is formed and nickel is completely alloyed already at 450 °C (indium phases cannot be detected after cooling down). This also means that In_2O_3 can be reduced fully below 450 °C. The Co bimetallic phase does not appear, and cooling down the sample to room temperature (i.e. below the melting point of In, 156.4 °C), the diffraction lines of indium particles are well detectable (compare b' and d' in Fig. 4a). In the case of Cu or Ni host metals, the formation of Cu_2In or Ni_2In phases were unequivocally detected in numerous studies [7–9, 13]. However, intermetallic compounds of cobalt with similar stoichiometry do not exist. Possible substances should be $CoIn_2$ or $CoIn_3$,—none of them could be detected by HT-XRD after adding a stoichiometrically sufficient amount of In_2O_3. However their formation as a skin in the external layer of the cobalt particles cannot be excluded.

In the diffractogram of NiX, strong reflections of crystalline Ni^0 appeared only at reduction temperature 650 °C (curve c in Fig. 4B). Unlike to the mesoporous silica support, carrying Ni-oxide particles, the nickel cations are distributed on the cationic sites of the faujasite framework compensating negative framework charge. Only a small fraction of nickel could be reduced at 450 °C (curve b in Fig. 4B). The residual Ni^{2+} lattice cations stabilized the structure of the aluminum-rich zeolite X. It was shown in an earlier study that zeolite CuX, containing easy-to-reduce copper ions, suffers complete structural collapse upon reduction under similar conditions [13]. The reduction of the nickel cations becomes complete at temperature only about 650 °C. The H-form of the zeolite X was generated that carried Ni^0 particles. In the absence of steam, the crystallinity of the zeolite was preserved to a significant extent. The average size of the Ni^0 particles, estimated by the Scherrer equation, was 17 nm. This infers that the catalytically active particles can be only on the outer surface of the micron-size zeolite crystals. The behavior of CoX heating up in the reducing atmosphere seems to be quite similar. The only difference is that cobalt particles are much smaller (13 nm) similarly to Co-form of SBA-15 supported catalysts.

In_2O_3 mixed with NiX or CoX could be also completely reduced up to 450 °C. Nevertheless, neither In nor the alloyed phases could be detected at any temperature of the XRD measurement. These results suggest that the indium must be present in highly dispersed form in the zeolite cavities and probably a small fraction of the introduced indium modified the active surface of the larger metal crystallites situated outside the micropores.

Monometallic nickel containing zeolite catalysts are very active in AA hydrogenolysis giving CH_4 and H_2O as products. Carbon dioxide and carbon monoxide might have been formed only as intermediate and are rapidly reduced to methane (see Fig. 5a). CoX seems to be more active and this is manifested significantly in much higher ethanol yield. Indium admission to both zeolite catalysts can completely eliminate the methane formation. The absence of CO as a

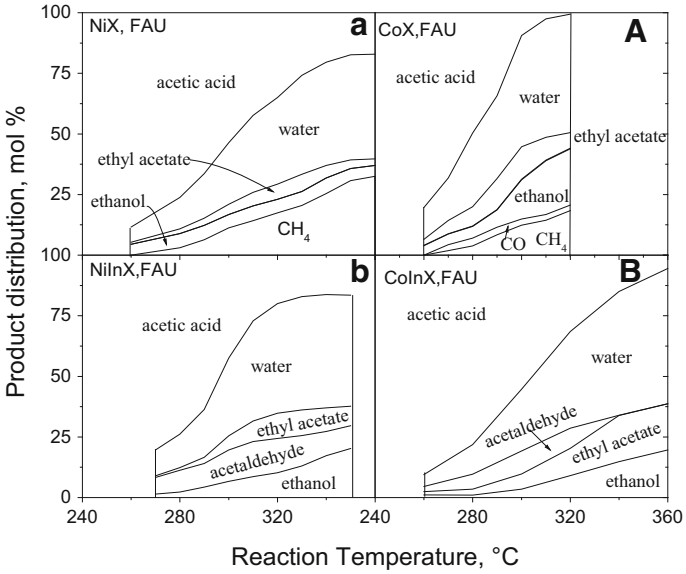

Fig. 5 Stacked area graphs representing product distribution of AA hydroconversion as a function of reaction temperature at 21 bar and 1 $g_{AA}/(g_{cat}.h)$ WHSV over (**a**, **A**) In-free and (**b**, **B**) In-modified catalysts. Support is zeolite X for Co (**A**, **B**) and Ni (**a**, **b**)

product also shows that the In-modified catalysts do not have hydrodecarbonylation activity. Similar effects of In-modification were reported in earlier studies [9, 13]. An important observation is that in the case of CoX after indium doping the complete improvement of selectivity is attached with significant decrease of the activity, i.e. full conversion can be attained only at higher temperature similarly to alumina supported Co-catalysts shown in a former study [14]. One of the possible explanations (simple geometric effect) is that cobalt atoms on the surface are much more diluted with indium because cobalt can form only $CoIn_2$ or $CoIn_3$ phases as intermetallic compounds contrary to Cu_2In or Ni_2In.

The SBA-15 supported catalysts were found to be significantly more active than the zeolite forms (Fig. 6) because the latter catalysts contained less active metal as the zeolitic cations are reduced to lower extent only at the routine pretreatment temperature. However, at higher temperature, aggregation can form larger metal particles with lower active surface on the outer surface of the zeolite crystallites. Surprisingly, acetaldehyde but not ethanol was formed over Ni/SBA-15 catalyst, whereas ethanol but no acetaldehyde was obtained as product when NiX catalyst was used. Methane as a useless by-product was the main product over both Ni-catalysts reflecting that on nickel AA hydrogenolysis is the preferred reaction path. On the contrary, on Co/SBA-15, the step by step consecutive reduction is the characteristic reaction feature excluding significant extent of methane production below 300 °C. The great advantage of monometallic Co/SBA-15 catalyst is that it enables to attain slight CH_4 yield accompanied with high activity and stability (see Fig. 7).

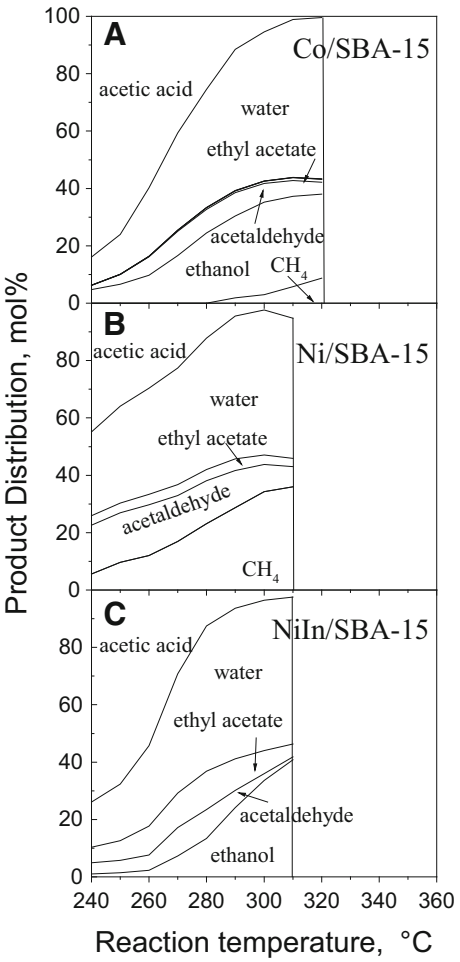

Fig. 6 Stacked area graphs of product distribution of AA hydroconversion as a function of reaction temperature at 21 bar and 1 $g_{AA}/(g_{cat}.h)$ WHSV over (**a**, **b**) In-free and (**c**) In-modified catalysts. Support is SBA-15 for Co (**a**) and Ni (**b**, **c**)

The selectivity change by using SBA-15 support is more pronounced than that of the zeolite catalysts after admission of indium. The modification with indium reduced the activity somewhat but did not affect the specific surface area of the catalysts. The TEM images show that the accessible surface area of the alloyed metal in the channels of the SBA-15 material hardly changes with the indium loading. Only the lengths of the nanowires, i.e. the inaccessible superficies grow. On Ni/SBA-15, the yield of intermediate product acetaldehyde and the ethyl acetate product of esterification are suppressed if more severe reaction conditions are applied. The main product ethanol and reactant acid can form ethyl acetate as a product of esterification, proceeding on a non-catalytic route. At higher reaction temperatures, the ester yield decreases indicating that the activation energy of ester hydrogenolysis is higher than that of ester formation. The simpler monometallic, unmodified Co/SBA-15 exceeds the properties of bimetallic NiIn/SBA-15 at lower reaction temperature. Furthermore, indium admission to cobalt catalysts results in

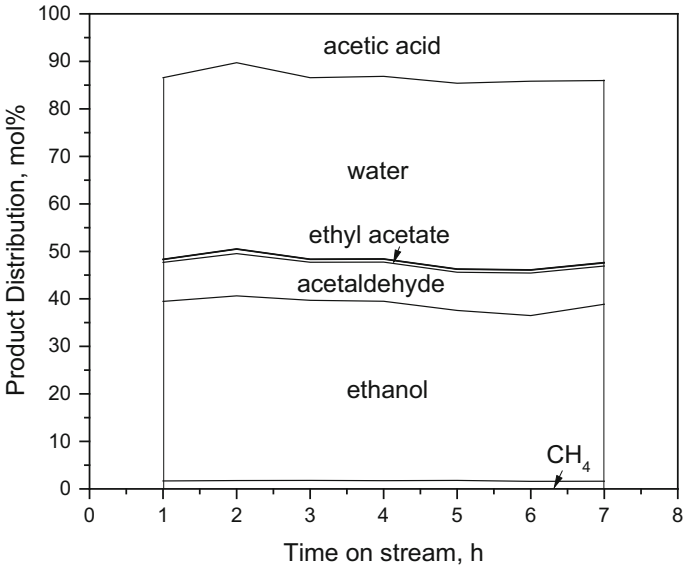

Fig. 7 Stacked area graphs of product distribution of AA hydroconversion as a function of time on stream at 290 °C and 1 $g_{AA}/(g_{cat.}h)$ WHSV over Co/SBA-15

lower activity (see for example in Fig. 5 for CoNiX, not shown for CoIn/SBA-15 in Fig. 6). In summary, the highly ordered mesopore system of the SBA-15 support may favor lower diffusional resistance and allows higher rate of transformation compared to microporous systems.

Conclusion

This study reveals that monometallic Co catalysts can be competitive with the most efficient bimetallic composites although under limited reaction conditions. Regarding both activity and ethanol selectivity, the mesoporous silica SBA-15 material was found to be more advantageous catalyst support than the microporous zeolite faujasite (presumably, the active metal particles can block a fraction of the channels in this support limiting the accessibility of the active metal surfaces). It was shown that In and Ni forms an alloy, which has the stoichiometry of Ni_2In. Alloying with In inhibited the hydrogenolysis activity of the supported Ni catalyst. The catalyst steered the acetic acid conversion in the direction of step-by-step reduction to ethanol by high selectivity. Indium doping essentially decreases the activity of Co in contrast to Ni. Co is not able to form Co_2In phase, only such intermetallic compounds are existing where the indium content is four or six times higher than in Cu or Ni composites.

Acknowledgements Thanks are due to the National Research, Development and Innovation Office, for supporting this research work from the National Research, Development and Innovation Fund (Grant No. TÉT_15_IN-1-2016-0034 and the Hungary-Slovakia Cross-border Co-operation Programme (Project registration number: HUSK/1101/1.2.1/0318).

References

1. Chang HN, Kim NJ, Kang JW, Jeong CM (2010) Biomass-derived volatile fatty acid platform for fuels and chemicals. Biotechnol Bioprocess Eng 15:1–10
2. Alonso DM, Wettstein SG, Dumesic JA (2012) Bimetallic catalysts for upgrading of biomass to fuels and chemicals. Chem Soc Rev 41:8075–8098
3. Alcala R, Shabaker JW, Huber GW, Sanchez-Castillo MA, Dumesic JA (2005) Experimental and DFT studies of the conversion of ethanol and acetic acid on PtSn-based catalysts. J Phys Chem B 109:2074–2085
4. Passos FB, Aranda DAG, Schmal M (1998) Characterization and catalytic activity of bimetallic Pt-in Al_2O_3 and Pt-Sn/Al_2O_3 catalysts. J Catal 178:478–488
5. Mohr C, Hofmeister H, Radnik J, Claus P (2003) Identification of active sites in gold-catalyzed hydrogenation of acrolein. J Am Chem Soc 125:1905–1911
6. Haass F, Bron M, Fuess H, Claus P (2007) In situ X-ray investigations on AgIn/SiO_2 hydrogenation catalysts. Appl Catal A 318:9–16
7. Onyestyák Gy, Harnos Sz, Kaszonyi A, Štolcová M, Kalló D (2012) Acetic acid hydroconversion to ethanol over novel InNi/Al2O3 catalysts. Catal Commun 27:159–163
8. Onyestyák Gy (2013) Outstanding efficiency of indium in bimetallic catalysts for hydroconversion of bioacids to bioalcohols. Catal Commun 38:50–53
9. Onyestyák Gy, Harnos Sz, Kalló D (2011) Improving the catalytic behavior of Ni/Al2O3 by indium in reduction of carboxylic acid to alcohol. Catal Commun 16:184–188
10. Rachmady W, Vannice MA (2000) Acetic acid hydrogenation over supported platinum catalysts. J Catal 192:322–334
11. Onyestyák Gy, Harnos Sz, Badari CA, Drotár E, Klébert Sz, Kalló D (2015) Acetic acid hydroconversion over mono-and bimetallic indium doped catalysts supported on alumina and silicas of various textures. Open Chem 13:517–527
12. Zhao D, Feng J, Huo Q, Melosh N, Fredrickson GH, Chmelka BF, Stucky GD (1998) Triblock copolymer syntheses of mesoporous silica with periodic 50 to 300 angstrom pores. Science 279:548–552
13. Onyestyák Gy, Harnos Sz, Kalló D (2013) Indium an efficient co-catalyst in novel Cu or Ni catalysts for selective reduction of biomass derived fatty acids to alcohols. In: Woo HG, Choi HT (eds) Indium: properties, technological applications and health issues, vol 2. Nova Science Publishers, New York
14. Onyestyák Gy, Harnos Sz, Kalló D (2015) Bioacid hydroconversion over Co, Ni, Cu mono- and indium-doped bimetallic catalysts. Acta Chim Slov 62:213–218